



## Correlation between non-collinear exchange coupling and interface structure in Fe/Cr(001) superlattices

A. Schreyer<sup>a,\*</sup>, J.F. Ankner<sup>b</sup>, M. Schäfer<sup>c</sup>, H. Zabel<sup>a</sup>, C.F. Majkrzak<sup>d</sup>, P. Grünberg<sup>c</sup>

<sup>a</sup> *Experimentalphysik/Festkörperphysik, Ruhr-Universität Bochum, 44780 Bochum, Germany*

<sup>b</sup> *Missouri University Research Reactor, Columbia, MO 65211, USA*

<sup>c</sup> *Forschungszentrum Jülich, 52425 Jülich, Germany*

<sup>d</sup> *National Institute of Standards and Technology, Gaithersburg, MD 20899, USA*

### Abstract

Using polarized neutron reflectometry with polarization analysis we have studied the non-collinear interlayer exchange coupling in Fe/Cr(001) superlattices as a function of growth temperature. From diffuse X-ray spectra we find that the occurrence of non-collinear spin structures is correlated with long range lateral Cr-thickness fluctuations which, in turn, depend on the growth temperature. This finding leads the way to a better understanding of the origin of non-collinear coupling in Fe/Cr(001).

The discovery of the now widely studied oscillatory exchange coupling between magnetic layers in artificially layered magnetic systems [1, 2] is one of the most interesting developments in modern magnetism. It came as a surprise when evidence was found that in addition to collinear ferromagnetic (FM) and antiferromagnetic (AF) coupling non-collinear 90° spin structures can also exist in simple transition metal layered structures [3, 4]. To account for the coupling angle of 90°, a second ‘biquadratic’ (BQ) exchange coupling term was postulated phenomenologically in addition to the conventional bilinear (BL) one [3]. Experimental evidence for the significance of this biquadratic term has been obtained for various systems (see e.g. the list of references in Ref. [5]).

It has been demonstrated theoretically that a biquadratic term can result from lateral long range thickness fluctuations of the interlayer [6], from paramagnetic impurities in the interlayer [5], and from the dipole exchange interaction between stepped interlayer interfaces [7]. In contrast to these ‘extrinsic’ mechanisms it was also shown that the biquadratic coupling term also results for ideal sample structures, i.e. intrinsically, as a second order term of the oscillatory first order Heisenberg exchange interaction [8].

Most recently Slonczewski has suggested a new Cr specific phenomenological model for non-collinear coupling [9] which is based on the assumption that the adjoining ferromagnets polarize the Cr interlayer, inducing an AF structure *above* the bulk Néel temperature of Cr (proximity magnetism). Proposing the existence of a helicoidally twisted quasi-antiferromagnetic structure of the Cr and assuming a lateral Cr thickness fluctuation on a length scale  $l^{\text{Cr}}$  Slonczewski arrives at a coupling energy which is completely different from the bilinear – biquadratic exchange energy used so far. Similar to Slonczewski’s first interlayer fluctuation based model [6] the proximity magnetism effect becomes important for large  $l^{\text{Cr}}$ , however it breaks down above a cut-off length  $l_{\text{co}}^{\text{Cr}} \approx 100 \text{ \AA}$  [9].

In this paper we present polarized neutron reflectometry (PNR) and off-specular X-ray data from Fe/Cr superlattices grown at two different temperatures. We find strong evidence for a correlation between non-collinear coupling and the existence of long range interlayer thickness fluctuations in the samples. This result leads the way to a better understanding of the origin of non-collinear coupling in this system.

Epitaxial Fe/Cr(001) superlattices were prepared by molecular beam epitaxy on a GaAs/Fe/Ag substrate–buffer system as described in Ref. [3]. In this paper we compare

\* Corresponding author.

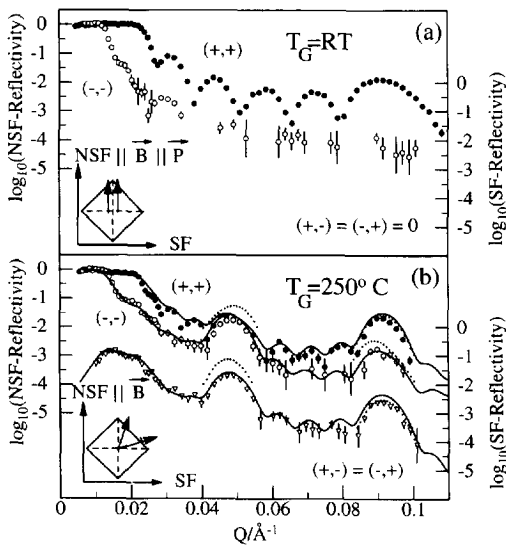


Fig. 1. (a) PNR data of the RT sample measured in  $B_{GF} = 17$  G parallel to an easy axis (dashed lines in the insets) after initial saturation. SF scattering was not detected in this case. (b) PNR NSF (top) and SF (bottom) data at  $B = 17$  G along an easy axis of the ET sample with calculations for coupling angles of  $50^\circ$  (lines) and  $90^\circ$  (small dots), respectively. The first case is depicted in the inset.

two superlattices, one grown at room temperature (RT) with 5 double layers and one at an elevated temperature (ET) of  $250^\circ$  with 9 double layers but otherwise with the same layer thicknesses (52 Å Fe and 17 Å Cr). These will be designated in the following as RT and ET.

To determine the magnetic structure, polarized neutron reflectivity (PNR) measurements have been performed on the reflectometer BT-7 at the NIST research reactor. Details can be found e.g. in Refs. [10–13]. All four reflectivities  $R(++)$ ,  $R(--)$ ,  $R(+,-)$ , and  $R(-,+)$  were measured and corrected for diffuse scattering. Here  $+$  ( $-$ ) designates the up (down) polarization of the incident and reflected neutrons, respectively. The first two non-spin flip (NSF) reflectivities contain information both on the chemical structure and on the projection of the magnetic in-plane moment *parallel* to the polarization vector  $\mathbf{P}$  of the incident neutrons, leading to a magnetic splitting of the otherwise degenerate  $R(++)$  and  $R(--)$ . The last two spin flip (SF) reflectivities, on the other hand, originate from any magnetization components *perpendicular* to  $\mathbf{P}$ . Thus, from a measurement and quantitative analysis of the NSF and SF reflectivities magnitude and orientation of the in-plane magnetic moments can be mapped out. It is useful to define the axes parallel and perpendicular to  $\mathbf{P}$  as the NSF and SF axes (see insets in Fig. 1).

In Fig. 1 (a) the PNR result of the RT sample is shown. The data were taken essentially in remanence after saturation in high fields. A small field of 17 G is required

to define  $\mathbf{P}$ . The field was applied parallel to one of the easy magneto crystalline [100] axes of Fe (dashed lines in the inset). A first order superlattice peak is seen at  $Q_{SL} = 2\pi/\Lambda_{nuc} = 0.09 \text{ \AA}^{-1}$  indicating that the magnetic and the nuclear periodicities are identical, as expected for a ferromagnetic alignment of the moments. The other four maxima between the critical scattering vector for total reflection and the superlattice peak are due to total film thickness oscillations from five superlattice periods. Moreover, the splitting between the  $(++)$  and  $(--)$  data and the absence of any intensity in the SF channel indicates alignment of all magnetic moments in the Fe layers parallel to the NSF direction, as indicated by the arrows in the inset.

In Fig. 1(b) we show PNR results of the ET sample, which were obtained in the same way as in the previous case. Clearly, the NSF reflectivities (plotted against the left hand axis) are split and additional strong SF scattering (plotted against the right-hand axis) is observed. All reflectivities exhibit first order superlattice peaks at  $Q_{SL} = 2\pi/\Lambda_{nuc} \approx 0.09 \text{ \AA}^{-1}$  originating from the superlattice's nuclear periodicity  $\Lambda_{nuc}$ . In addition, half-order peaks at about  $Q_{SL}/2$  are observed in all reflectivities. These result from a doubling of the magnetic periodicity over the nuclear one, as would be seen in a collinear AF structure. Such an AF structure has no resulting moment. However, the splitting of the NSF data and the existence of a first-order peak in the SF data clearly indicate that a finite moment is projected along the NSF and SF axes in every layer. Therefore, the half-order peaks can only be caused by a non-collinear moment orientation [14]. The simplest assumption would be a perpendicular orientation of the moments along the two easy axes (dashed lines). Nevertheless, the calculated SF and NSF reflectivities for this magnetic structure (small dots in Fig. 1(b)) show that the data are not consistent with such a  $90^\circ$  model [15]. On the other hand, if non-perpendicular orientation is allowed, the data can be well fitted (solid line in Fig. 1(b)) by assuming a coupling angle of  $\varphi_c = 50^\circ \pm 4^\circ$  between the adjacent Fe layers, as schematically depicted by the solid arrows in the inset of Fig. 1(b). Input to the model calculation is the sample structure as determined from fits to X-ray data and the Fe magnetic moment as found by PNR in the saturated state. The only fit parameters left are the *orientations* of the moments in the Fe layer [18]. These results were confirmed by additional PNR scans for different sample orientations in which only  $\varphi_c$  was varied [17].

Comparison of Figs. 1(a) and (b) clearly shows that the different growth temperature of the otherwise equivalent Fe/Cr superlattices has a dramatic effect on the exchange coupling between the Fe layers.

To understand this effect, the samples were characterized with X-rays by specular and off-specular (diffuse) small angle reflectivity, high angle Bragg scattering, and grazing incidence diffraction. No indication of any difference in

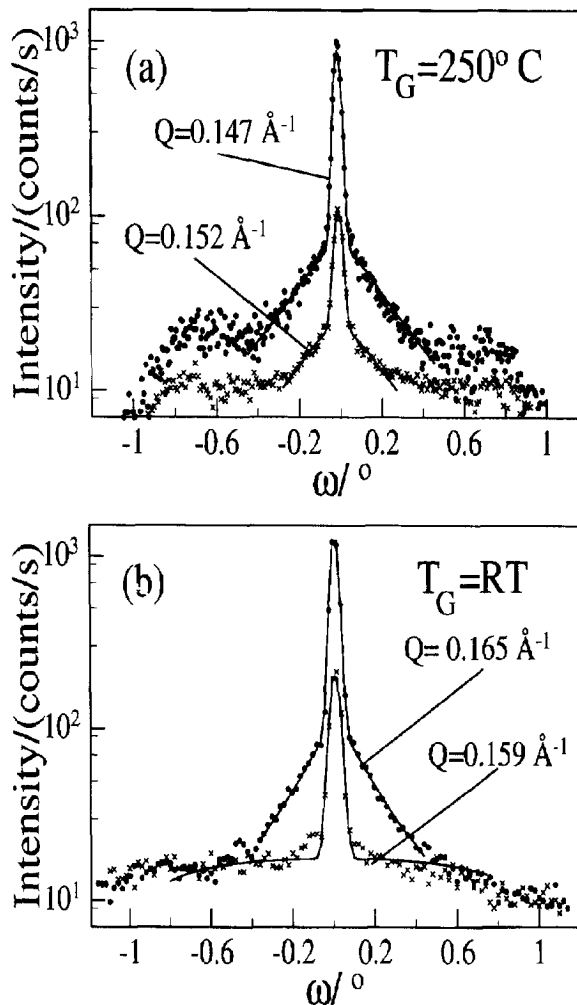


Fig. 2. Small angle rocking curves of the ET (a) and RT (b) samples measured through two adjacent maxima (dots) and minima (crosses) of the finite thickness oscillations at the  $Q$  indicated with fits, as detailed in the text.

crystalline structure as a function of the growth temperature  $T_G$  was obtained. Fits to the high angle and the small angle specular reflectivity data indicate small interface roughnesses  $\sigma$ , defined as the rms deviation  $\sqrt{\langle z^2 \rangle}$  from the ideal interface, in the range of 0.5 to 2.5 monolayers (0.7–3.6 Å) [17]. In general, the samples grown at 250°C exhibit larger rms roughnesses than the ones grown at RT.

Strong evidence for another distinct structural difference was found from the off-specular (diffuse) scattering [19, 20] in the small angle reflectivity regime. Fig. 2 shows rocking curves through adjacent maxima (dots) and minima (crosses) of the finite thickness oscillations. In three of the four scans diffuse cusps, which are symmetric with respect to the specular peak at  $\omega = 0$ , are found. Only in the scan through the minimum shown in Fig. 2(b) a much

broader feature is observed. The width of the diffuse cusps is inversely related to the length scale of lateral correlations of the interfaces. The scans through the minima (crosses) indicate the presence of a vertically uncorrelated *short* length scale lateral interface fluctuation for growth at RT (Fig. 2(b)), whereas for growth at 250° we find a *long* length scale uncorrelated interface fluctuation (Fig. 2(a)). In both cases these *uncorrelated* fluctuations are superimposed on long length scale vertically *correlated* interface fluctuations, as evidenced by the diffuse scattering in the transverse scans through the maxima (dots). Since any *uncorrelated* interface fluctuation translates into a layer thickness fluctuation in the sample plane, the data provides evidence for a significant difference in the lateral length scale  $l$  of the fluctuation of the layer thicknesses as a function of  $T_G$ . Quantitative analysis [19] of the data yields the rough estimates  $l_{RT}^c \leq 10$  Å and  $l_{ET}^c \approx 100$  Å [17].

Thus, comparison of Figs. 1 and 2 indicates a correlation between the occurrence of non-collinear coupling and long range Cr layer thickness fluctuations. This result provides strong evidence for the dominance of those two mechanisms of non-collinear coupling in Fe/Cr [6, 9] which are based on long length scale interlayer thickness fluctuations. However, it remains to be clarified which of these two mechanisms is more appropriate. This amounts to distinguishing between a bilinear-biquadratic and the non-trigonometric exchange energy postulated by Slonczewski for his new proximity magnetism model. For this purpose field dependent PNR and magneto optic Kerr effect measurements have been performed. These are presented elsewhere [17, 21].

In conclusion, we have demonstrated the use of PNR with polarization analysis for determining the coupling angle of non-collinearly coupled systems. Hardly any other method can provide this wealth of information on the magnetic structure of such systems. Surprisingly, a significant deviation from the perpendicular moment orientation reported before [3] is found [22]. Measurements of the diffuse X-ray scattering of collinearly and non-collinearly coupled samples yields strong evidence that lateral long range Cr interlayer thickness fluctuations are responsible for the non-collinear coupling in Fe/Cr(001). This result provides the basis for a more detailed understanding of non-collinear coupling in this system [17].

We acknowledge financial support by the German BMBF (ZA03BOC) and DFG (SFB166) for the work in Bochum, as well as a travel grant from NATO (CRG901064).

## References

- [1] For a review on transition metal systems see e.g.: B. Heinrich and J.F. Cochran, Adv. Phys. 42 (1993) 523.

- [2] For a review on rare earth systems see: C.F. Majkrzak et al., *Adv. Phys.* 40 (1991) 99.
- [3] M. Rühlig et al., *Phys. Stat. Sol. (A)* 125 (1991) 635.
- [4] B. Heinrich et al., *Phys. Rev. B* 44 (1991) 9348.
- [5] J.C. Slonczewski, *J. Appl. Phys.* 73 (1993) 5957.
- [6] J.C. Slonczewski, *Phys. Rev. Lett.* 67 (1991) 3172.
- [7] S. Demokritov et al., *Phys. Rev. B* 49 (1994) 720.
- [8] For the intrinsic mechanism see e.g. R.P. Erickson, K.B. Hathaway and J.R. Cullen, *Phys. Rev. B* 47 (1993) 2626 or the list of references in Ref. [5].
- [9] J.C. Slonczewski, *J. Magn. Magn. Mater.*, to be published.
- [10] C.F. Majkrzak, *Physica B* 173 (1991) 75.
- [11] G.P. Felcher, *Physica B* 192 (1993) 137.
- [12] H. Zabel, *Physica B* 198 (1994) 156.
- [13] A. Schreyer et al., *J. Appl. Phys.* 73 (1993) 7617.
- [14] J.F. Ankner et al., in: *Magnetic Ultrathin Films, Multilayers and Surfaces*, eds. C. Chappert et al., MRS Symposia Proceedings (Materials Research Society, Pittsburgh, 1993) Vol. 313, p. 761.
- [15] As discussed in an earlier version of the fitting [16], a mixed coherent–incoherent averaging over two types of domains was assumed in order to reproduce the data for a  $90^\circ$  domain model. However, this model fails when applying to the field dependence of the spin structure, as discussed elsewhere [17].
- [16] A. Schreyer et al., *Physica B* 198 (1994) 173.
- [17] A. Schreyer et al., *Europhys. Lett.* 32 (1995) 595. A. Schreyer, PhD Thesis, Ruhr-Universität Bochum (1994).
- [18] As detailed elsewhere [17] domains only complicate the modeling close to remanence. However, even here only two types of domains, which differ in stacking sequence, are found. These do not affect the modeling in any significant way.
- [19] For methodical details see e.g. D.E. Savage et al., *J. Appl. Phys.* 69 (1991) 1411.
- [20] W. Press et al., *Physica B* 221 (1996) 1.
- [21] From these results strong evidence for the validity of the proximity magnetism effect for our samples with an intermediate  $l_{\text{ET}}^{\text{Cr}} \simeq 100 \text{ \AA}$  is inferred, providing an explanation for the occurrence of the observed non-collinear coupling [17]. On the other hand, samples grown at similar temperatures on different substrates (Fe whiskers) with the same Cr interlayer thickness show purely FM coupling (see for example Ref. [1]). In this case  $l^{\text{Cr}}$  is much larger [1] than the cut-off length of the proximity magnetism effect. Thus for large and small  $l^{\text{Cr}}$  (see above) FM coupling is observed for this Cr interlayer thickness, whereas for an intermediate  $l_{\text{ET}}^{\text{Cr}} \simeq 100 \text{ \AA}$  non-collinear coupling is found due to proximity magnetism.
- [22] The samples discussed in Ref. [3] were grown at RT. Furthermore, the perpendicular moment orientations were found for different Cr interlayer thicknesses. Thus, these results cannot directly be compared with those presented here.